V. MICROWAVE ELECTRONICS

Prof. L. J. Chu
Prof. H. A. Haus
Prof. L. D. Smullin
A. Bers
T. J. Connor
B. W. Faughnan
C. Fried
C. Morgenroth
W. Schwab

A. EXPERIMENTAL DETERMINATION OF THE LONGITUDINAL INTRINSIC EMISSION NOISE CHARACTERISTICS OF AN ELECTRON BEAM AT MICROWAVE FREQUENCIES

The theory of noise in electron beams, subject to some restrictive assumptions, indicates two parameters of importance (1):

1. Π, the real part of the cross power density spectrum, CPDS, between the kinetic voltage and current fluctuations, representing noise kinetic power in the electron stream and

2. $S^2 = \Phi\Psi - \Lambda^2$ (1)

where Φ is the self power density spectrum, SPDS, of the fluctuations in kinetic voltage of the electrons, Ψ is the SPDS of the fluctuations in beam current, and Λ is the imaginary part of the CPDS between the fluctuations in kinetic voltage and current. Both of these quantities are conserved whenever the electrons are passed through regions in which no real electromagnetic power is extracted from, or delivered to, the electron beam.

1. Theory of Measurements: The Measurement of S

In a drift region where the electrons move under the action of the same dc electric field at all cross sections the power density spectra Φ and Ψ behave as standing waves along the drifting beam, and

$$S^2 = Z_o^2 \Psi_{max} \Psi_{min} \tag{2}$$

where $Z_o = \frac{2V_o}{I_o}\frac{\omega_q}{\omega}$ is the characteristic impedance of the drifting beam. S is thus seen to be related to the original Pierce-Bloom-Peter invariant noise parameter. From an experimental plot of noise current (in db below shot noise) versus distance along the drifting beam, S is given by

$$S = \frac{e}{\pi}\frac{V_o}{a}\frac{\lambda_e}{\lambda_q} \tag{3}$$

where e is the charge of an electron, V_o is the drift voltage of the electrons, $\lambda_e = \lambda \frac{V_o^{1/2}}{505}$ is the electron wavelength at the operating λ and beam voltage V_o, λ_q is the plasma wavelength, and a is given by $A = 10 \log_{10} a$, A being the average, in db below shot noise, of the noise current standing wave.

2. Theory of Measurements: The Measurements of Π

The action of a lossy beam network (one which can extract or deliver real electromagnetic power to the electron beam) upon the noise standing wave produces two measureable effects. The average of the standing wave (and hence S) and the standing wave ratio ρ^2, before and after the lossy network, will in general be different, the difference depending upon Π. We choose for our lossy beam network a resonant cavity through which the beam is passed in such a way as to interact with longitudinal (i.e., along the path of the beam) electric fields. A re-entrant-type cavity, common in klystron amplifiers, was used for actual measurements. A detailed theoretical analysis is given in (2) and will be published in a technical report. We shall summarize only the important results.

With the cavity placed at the position of maximum of the noise-current standing wave, which results in a maximum effect upon the standing wave, the SWR $\rho^2 = \frac{\Psi_{max}}{\Psi_{min}}$ changes in the following manner

$$\frac{1}{\rho_2^2} = \frac{1}{\rho_1^2} + M^4 \frac{Y_o^2}{|Y|^2} - 2M^2 \frac{Y_o}{G} \left[\frac{\Pi_1}{S_1} - \frac{kT}{2\pi S_1}\right] \frac{1}{\rho_1} \tag{4}$$

where ρ_1^2 and ρ_2^2 are SWR's before and after the cavity, respectively, Y_o is the characteristic admittance of the beam, Y and G are the admittance and conductance, respectively, of the cavity as seen by the electrons, and M is the beam-coupling coefficient. Under conditions of actual measurement the cavity and detection system are of finite bandwidths. Equation 4 must then be properly integrated over frequency. This gives

$$\frac{1}{\rho_2^2} = \frac{1}{\rho_1^2} + M^4 \frac{Y_o^2}{G^2} F - 2M^2 \frac{Y_o}{G} F \left[\frac{\Pi_1}{S_1} - \frac{kT}{2\pi S_1}\right] \frac{1}{\rho_1} \tag{5}$$

where F is a function characterizing the frequency dependence of the cavities and measuring system. For the case of tuned cavities and measuring system, all having the same frequency characteristics, F = 1/2.

3. Experimental Results

The ultimate minimum noise figure of a longitudinal-beam microwave amplifier is (1)

$$F_{min} = 1 + \frac{2\pi}{kT} (S-\Pi) \tag{6}$$

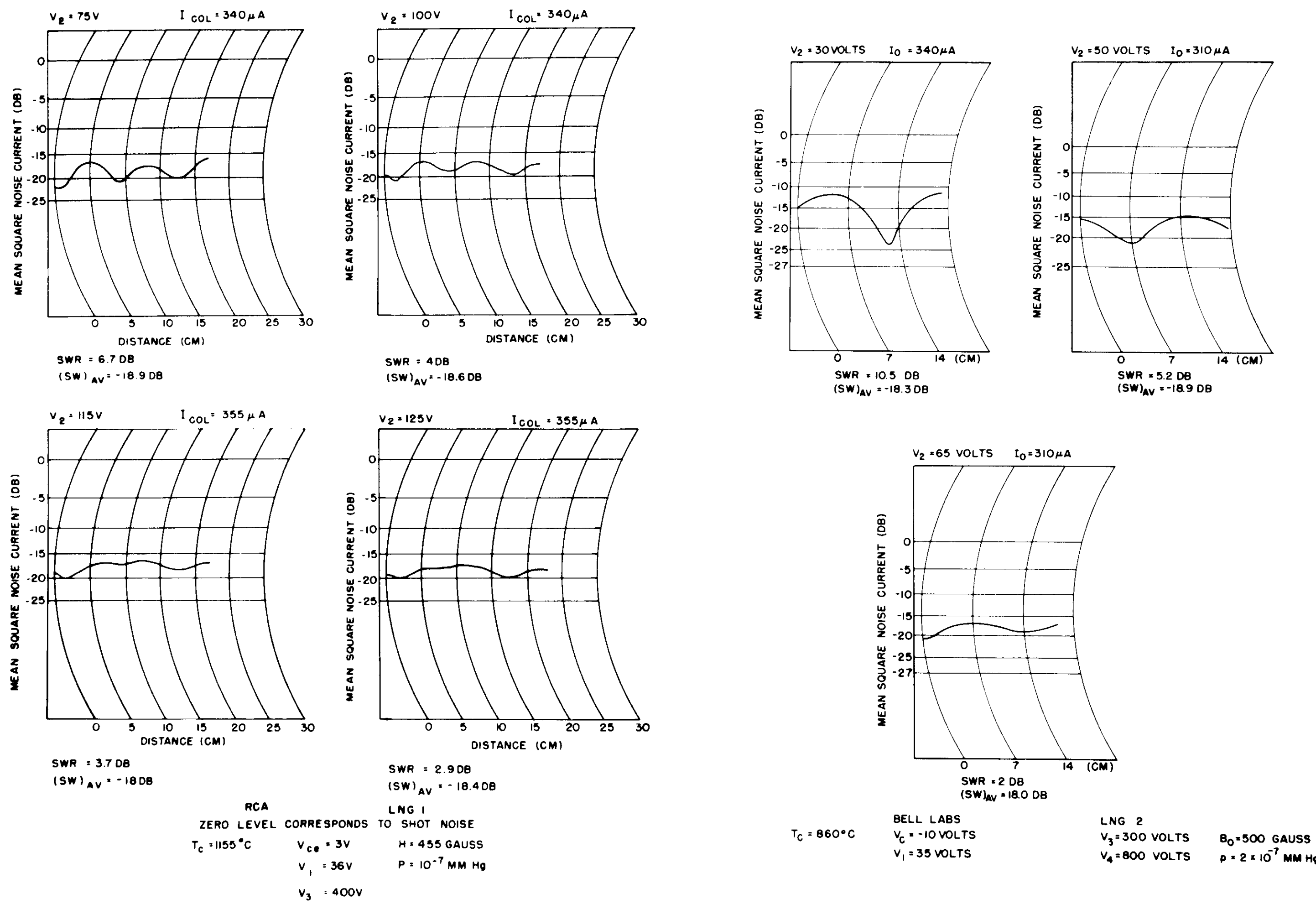

Fig. V-1. Noise current versus distance. Second anode voltage varied.

We recognize that in $(F_{min} - 1)$ the noisiness of the beam $(S-\Pi)$ is contrasted with the power density spectrum of an available thermal noise, $\theta = \frac{kT}{2\pi}$,

$$\frac{S-\Pi}{\frac{kT}{2\pi}} = \frac{S-\Pi}{\theta} = \frac{S}{\theta}\left(1 - \frac{\Pi}{S}\right) \tag{7}$$

We choose, therefore, to indicate experimental measurements through $\frac{S}{\theta}$ and $\frac{\Pi}{S}$ (for $T = 300°K$, $\theta = 6.59 \times 10^{-22}$ watt-sec).

In all measurements, confined-flow low-noise guns, having multiple (3-4) accelerating regions, were used. All the guns employed cathodes of 0.025-inch diameter. Throughout the measurements, interception current was less than 0.1 per cent of the total current. The technique of the sliding cavity noise pickup, and the radiometer detection system that was used are described elsewhere (2).

Figure V-1 shows experimental data of electron beam noise as a function of distance for two different low-noise guns. The RCA gun had an L-type impregnant cathode, while the Bell Telephone Laboratories gun had an oxide-coated cathode. The various standing waves were obtained by varying the second anode voltage. For all cathodes, two oxide-coated and three L-type impregnant, that were tested, the range of values obtained for the noise parameter S was approximately

$$3 \times 10^{-21} \leqslant S \leqslant 10 \times 10^{-21} \quad \text{watt-sec}$$

or

$$6.5 \leqslant \frac{S}{\theta} \leqslant 12 \quad \text{db}$$

In all measurements, on each particular gun and cathode, the average of the standing wave of noise, in db below shot noise, varied by ± 0.5 db. Hence the noise parameter S could be specified at best to within ± 12 per cent.

The experiments for the determination of Π were performed on a system shown schematically in Fig. V-2. The experiment consisted in first, measuring with the first cavity the noise current standing wave along the beam as it emerged from the low-noise gun; then, the first cavity was terminated in a matched load and fixed in position on a

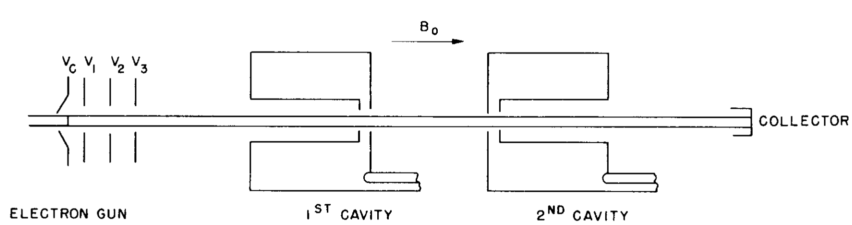

Fig. V-2. Experimental setup of system for determination of Π

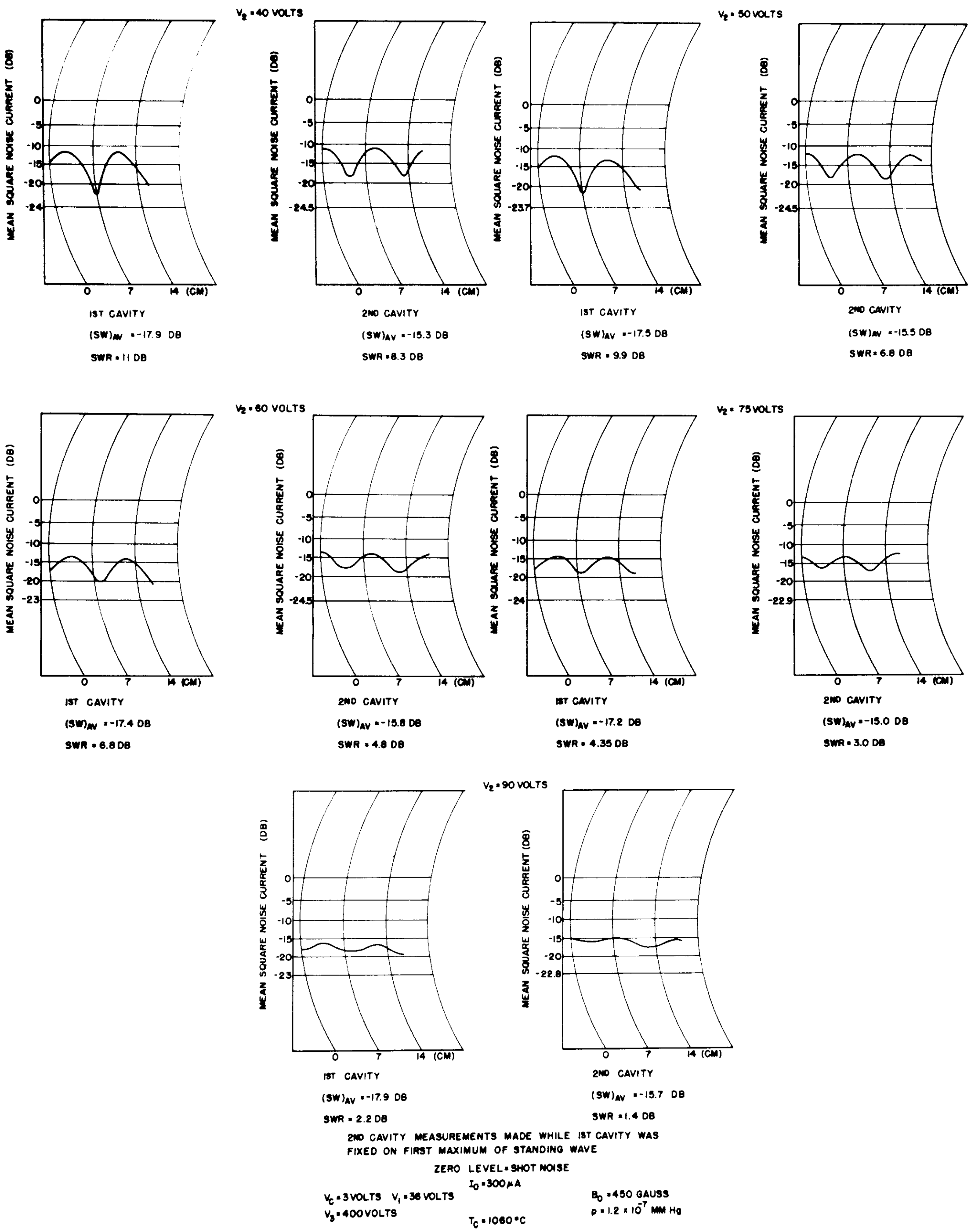

Fig. V-3. Noise current versus distance. Standing wave transformation by a cavity (35 hours after cathode activation).

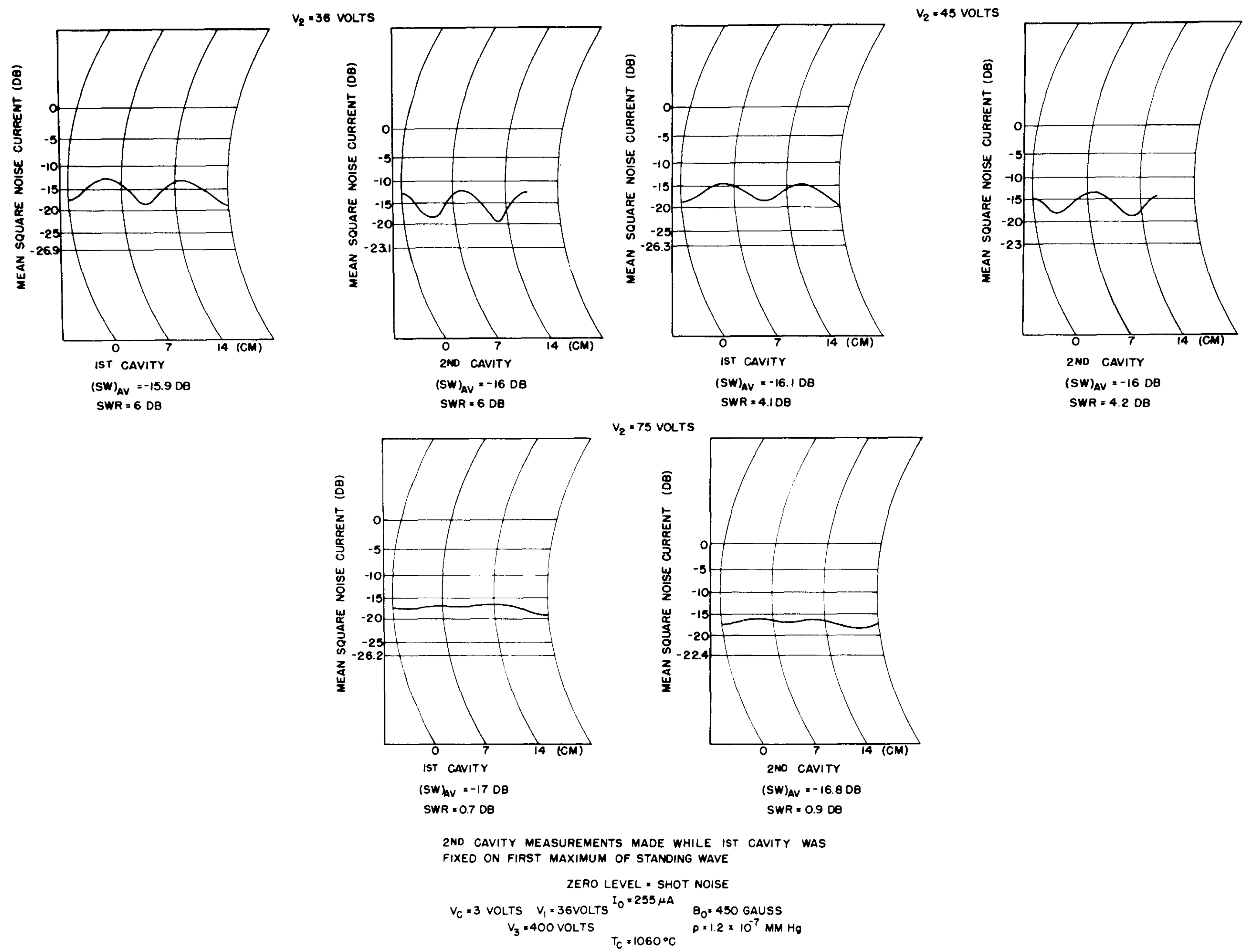

Fig. V-4. Noise current versus distance. Standing wave transformation by a cavity (100 hours after cathode activation).

current maximum of the standing wave, and the noise current following the first cavity was measured with the second cavity.

The experimental curves obtained from these measurements are shown in Figs. V-3 and V-4. An L-type cathode was used in the low-noise gun. The experimental data shown in these figures were taken on one and the same gun. Current was drawn from the cathode continuously from the time of activation until the completion of all experiments. Figure V-3 shows data that were taken about 35 hours after activation of the cathode, while the data shown in Fig. V-4 were taken about 65 hours later.

The various SWR's for which the experiment was performed were obtained by varying the second anode voltage, as in the case of the measurements of S. The characteristics of the measuring system that enter into Eq. 5 were determined by measurement. From our two sets of data we then obtain:

Table V-1

35 hours after activation
(I_o = 300 μa)

$$\text{Av. } \frac{\Pi_1}{S_1} = -0.31$$

with a variation of

$$-0.45 \leqslant \frac{\Pi_1}{S_1} \leqslant -0.14$$

Table V-2

100 hours after activation
(I_o = 255 μa)

$$\text{Av. } \frac{\Pi_1}{S_1} = +0.33$$

with a variation of

$$+0.32 \leqslant \frac{\Pi_1}{S_1} \leqslant +0.35$$

Equation 5 and data are plotted in Fig. V-5 and Fig. V-6 with Π/S as parametric curves in the allowable range of $\Pi/S = \pm 1$.

It should be noted that the first set of measurements was taken during the ageing period of the cathode. The measurements were started with high SWR's and finished at low SWR's. Hence the observed trend of increasing Π/S went along with increasing ageing time of the cathode. In the case of the fully-aged cathode the consistency in the measurement of Π/S is seen to be very good. The estimated possible error in the determination of each Π/S is about ±15-20 per cent.

A. Bers

References

1. H. A. Haus and F. N. H. Robinson, The minimum noise figure of microwave beam amplifiers, Proc. IRE 43, 981 (1955).
2. A. Bers, Experimental and theoretical aspects of noise in microwave tubes, S. M. Thesis, Department of Electrical Engineering, M.I.T., 1955.

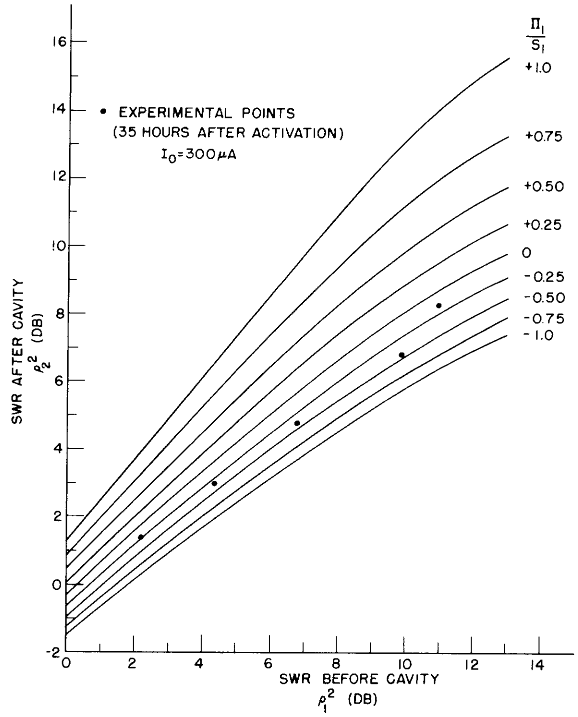

Fig. V-5. Noise current SWR transformation by a cavity

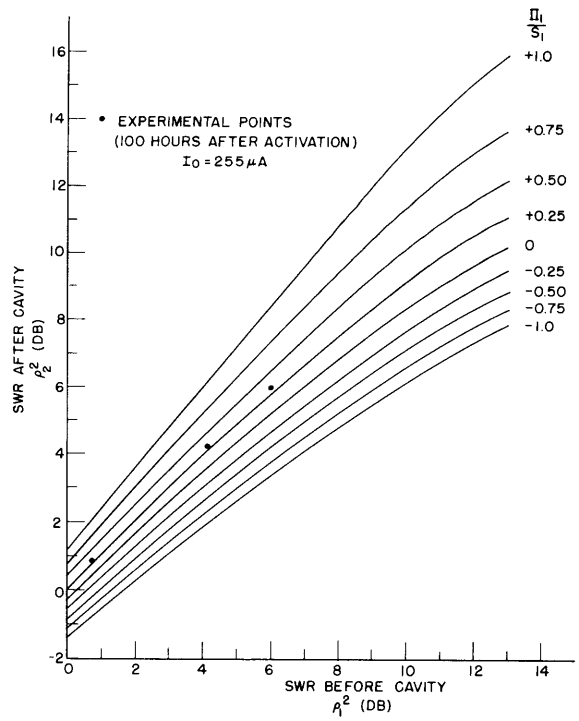

Fig. V-6. Noise current SWR transformation by a cavity

B. KLYSTRON AMPLIFIER NOISE FIGURE

An analysis of the minimum noise figure of a small-signal klystron amplifier has been carried out. The minimum noise figure of a klystron with infinitesimally short cavity gaps was found to be

$$F_{min} = \left(1 + \frac{G_s}{G_{gen}}\right)\left[1 + \frac{2\pi}{kT}(s - \Pi)\right]$$

Details of the analysis are given elsewhere (1), and will be published soon.

A. Bers

References

1. A. Bers, Experimental and theoretical aspects of noise in microwave tubes, S. M. Thesis, Department of Electrical Engineering, M.I.T., 1955.

C. MICROWAVE NOISE MEASUREMENTS WITH A RADIOMETER

The most widely used microwave noise source is the fluorescent lamp. Although it is very simple to use, its calibration by signal-generator methods is a tedious task. It was decided, therefore, to measure the microwave noise power of a fluorescent lamp by comparison against resistors held at known temperatures. Since the resistors could be operated conveniently only at low temperatures (boiling water down to liquid nitrogen) it was necessary to use a Dicke radiometer (1) as the comparison instrument. The

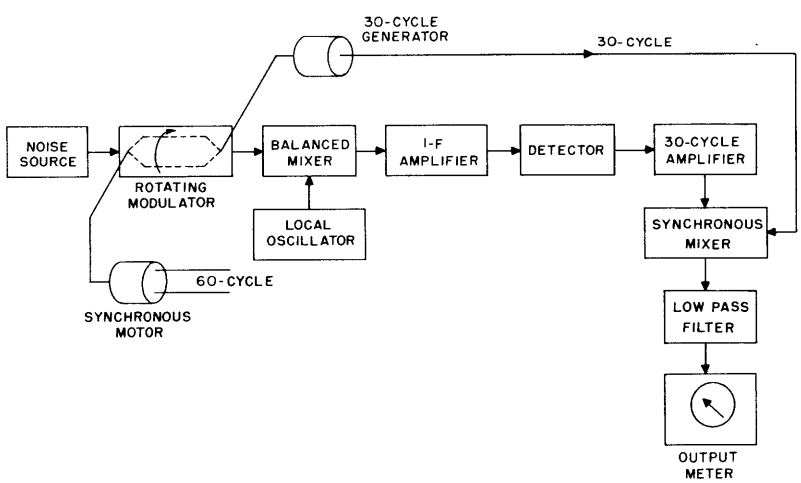

Fig. V-7. Microwave radiometer

measurements were made at 3000 Mc/sec. A more complete treatment will be found in (2).

1. Description of the System

For illustrative purposes consider the system of Fig. V-7. An absorbent attenuator wheel is made to rotate inside a section of waveguide so that the noise power entering the system alternates between that of the unknown noise source and the $KT\Delta f$ noise generated by the wheel itself. If there is an effective noise temperature difference between the unknown source and the reference, the detected output from the i-f amplifier contains not only noise but a signal at a frequency determined by the speed of rotation of the modulator. This signal and the attendant noise are then mixed with a synchronous reference signal of the proper phase relationship to yield a dc output plus noise, which is filtered and read directly on a meter. The dc term is related to the difference in source temperatures in both magnitude and sign. The noise accompanying the dc term contributes a slow fluctuation to the output, thus limiting the sensitivity. Another factor which can limit the sensitivity is the gain stability of the system.

2. Theoretical Sensitivity

The quality of a given radiometer system is most readily measured in terms of the incremental sensitivity, i.e., the smallest change, ΔT, that can be measured for a given temperature difference between reference and unknown. The criterion for measurability is an incremental signal-to-noise ratio of unity. Results for systems making use of both full-wave square-law and half-wave linear detectors were derived. In the analysis the effect of the slow gain fluctuation of the i-f amplifier was accounted for by assuming that the gain varied as $\left[1 + \alpha(t)\right]$; where $\alpha(t)$ is a Weikoff process and $\overline{\alpha^2(t)}$ is small. The sensitivity of the full-wave square-law detector is expressed by

$$\delta T_S = \frac{\pi^{3/2}}{4}\left[\frac{a}{\Delta\omega}\right]^{1/2}\left\{\left[\frac{32\overline{\alpha^2}\,\Delta T^2\,\Delta\omega}{\pi^3}\right]\left[\frac{2a^3 + \beta(\beta^2 - 3a^2)}{(\beta^2 - a^2)^2}\right] + \left[1 + 6\overline{\alpha^2}\right]\left[\Delta T^2 + (FT_r + \Delta T)^2\right]\right\}^{1/2} \tag{1}$$

and of the half-wave linear detector by

$$\delta T_L = \frac{\pi^{3/2}}{4}\left[\frac{a}{\Delta\omega}\right]^{1/2}\left[FT_r + \Delta T\right]\left[1 + \frac{\Delta T}{FT_r + \Delta T}\right]^{1/2}\left\{\left[1 + \overline{\alpha^2}\right]\right.$$

$$\left. + \left[1 - \sqrt{1 - \left(\frac{\Delta T}{FT_r + \Delta T}\right)^2}\,\right]\left[\frac{2a^3 - \beta(\beta^2 - 3a^2)}{(\beta^2 - a^2)}\right]\left[\frac{16\Delta\omega\overline{\alpha^2}}{\pi^3}\right]\right\}^{1/2} \qquad (2)$$

a = bandwidth of critical damping circuit low pass filter = 0.4 $\sec^{-1}$

$\Delta\omega$ = bandwidth of i-f amplifier = $4\pi \times 10^6$ $\sec^{-1}$

F = noise figure of i-f and mixer = 9.45 db

T_r = temperature of modulator reference wheel = 300°K

ΔT = temperature difference between unknown and reference

β = bandwidth of spectrum of $\alpha(t)$ fluctuations

The inclusion of the effect of gain fluctuation is of importance because it shows that the sensitivity cannot be made infinite by increasing the bandwidth.

Considering $\alpha^2(t) = 0$ and letting $\Delta T = 0$ yields the minimum value for δT_S. For the above parameter values $\delta T_S = 0.65$°K which corresponds to a minimum detectable power of 4×10^{-17} watts. The measured sensitivity agreed very favorably with the calculated value. The theoretical sensitivity was computed assuming a square-wave modulation of the noise. The modulator actually used gave a modulation with less power in the 30-cycle component by a factor of approximately 2. Comparison with Fig. V-8 shows indeed that the output fluctuations were of the order of 1.3°K.

If the bandwidth is made infinite and β is assumed much smaller than a, the worst possible condition, the limiting sensitivity becomes

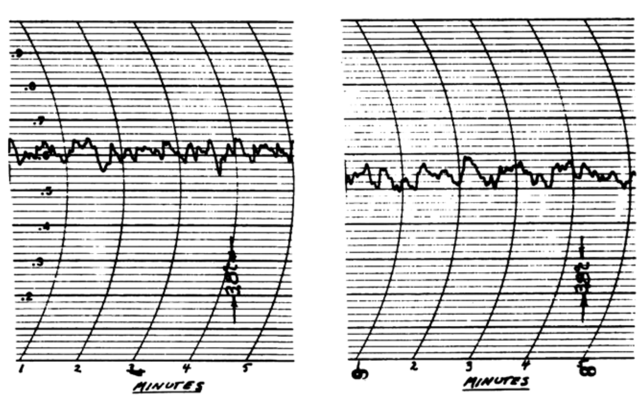

Fig. V-8. Radiometer output meter fluctuations. Typical samples taken on different days. rms fluctuation = 1°C.

Table V-3

Results of Measurements

Lamp No. dc	10 log T/290 50 ma	100 ma (Rated Current)	150 ma
1	16.12	16.02	15.87
2	15.87	15.94	15.78
3	16.03	16.02	15.96
4	15.96	16.00	15.98
5	16.08	16.04	15.93
6	15.88	15.80	15.63
7	16.06	16.04	15.91
8	15.92	15.96	15.72
9	16.08	16.04	16.03
10	16.08	16.06	16.00
11	16.00	16.04	15.97
12	15.98	15.96	15.82
13	16.04	16.01	15.98
14	16.04	15.95	15.92
15	16.07	16.02	15.94
16	16.04	15.97	15.89
17	16.16	16.11	16.06
18	16.04	15.94	15.88
Mean	16.03	15.99	15.90

Table V-4

Summary of Experimental Results

Lamp Current dc	Noise Temperature T Mean	Range	10 log T/290 Mean	Range
50 ma	11,611°K	11,850°K	16.03 db	16.16 db
		11,212		15.87
100 ma (Rated Current)	11,540	11,705	15.99	16.11
		11,020		15.80
150 ma	11,294	11,628	15.90	16.06
		10,598		15.63

Calculated rms Experimental Error = 90°K

$$\delta T_{S\,\substack{\Delta\omega\to\infty \\ \beta<a}} = 2\sqrt{\overline{a^2}}\,\Delta T \tag{3}$$

$$\delta T_{L\,\substack{\Delta\omega\to\infty \\ \beta<a}} = \sqrt{\overline{2a^2}}\left[FT_r + \Delta T\right]\left[1 + \frac{\Delta T}{FT_r + \Delta T}\right]^{1/2}\left[1 - \sqrt{1 - \left(\frac{\Delta T}{FT_r + \Delta T}\right)^2}\right]^{1/2} \tag{4}$$

Equations 3 and 4 indicate that in theory a null measurement technique can be used to obtain very accurate results.

3. Calibration

The noise temperature of a group of small-sized fluorescent lamps was measured by the radiometer system which had initially been calibrated quite accurately by using a special, matched, 7/8-inch, 50-ohm coaxial load and temperature baths with temperatures known accurately from physical laws.

The results of measurements on 18 standard 8-watt fluorescent lamps indicate that the noise temperature is 15.95 ±0.15 db above 290°K at rated current. The dependence of noise temperature on lamp conduction current was also noted. The experimental accuracy in measurement was 90°K rms. This represents an error in the value of the measured temperatures of approximately 0.08 per cent or 0.04 db. This error is mainly attributable to the inaccuracy in the attenuator inserted between the unknown load and the system.

The experimental data are shown in Tables V-3 and V-4.

W. C. Schwab

References

1. R. H. Dicke, Report 787, Radiation Laboratory, M.I.T. (1945).
2. W. C. Schwab, Analysis and calibration of an S-band radiometer, S. M. Thesis, Department of Electrical Engineering, M.I.T. (1955).